

Supplementary File

Figures S1 through S23 provide additional details related to the main text illustrations.

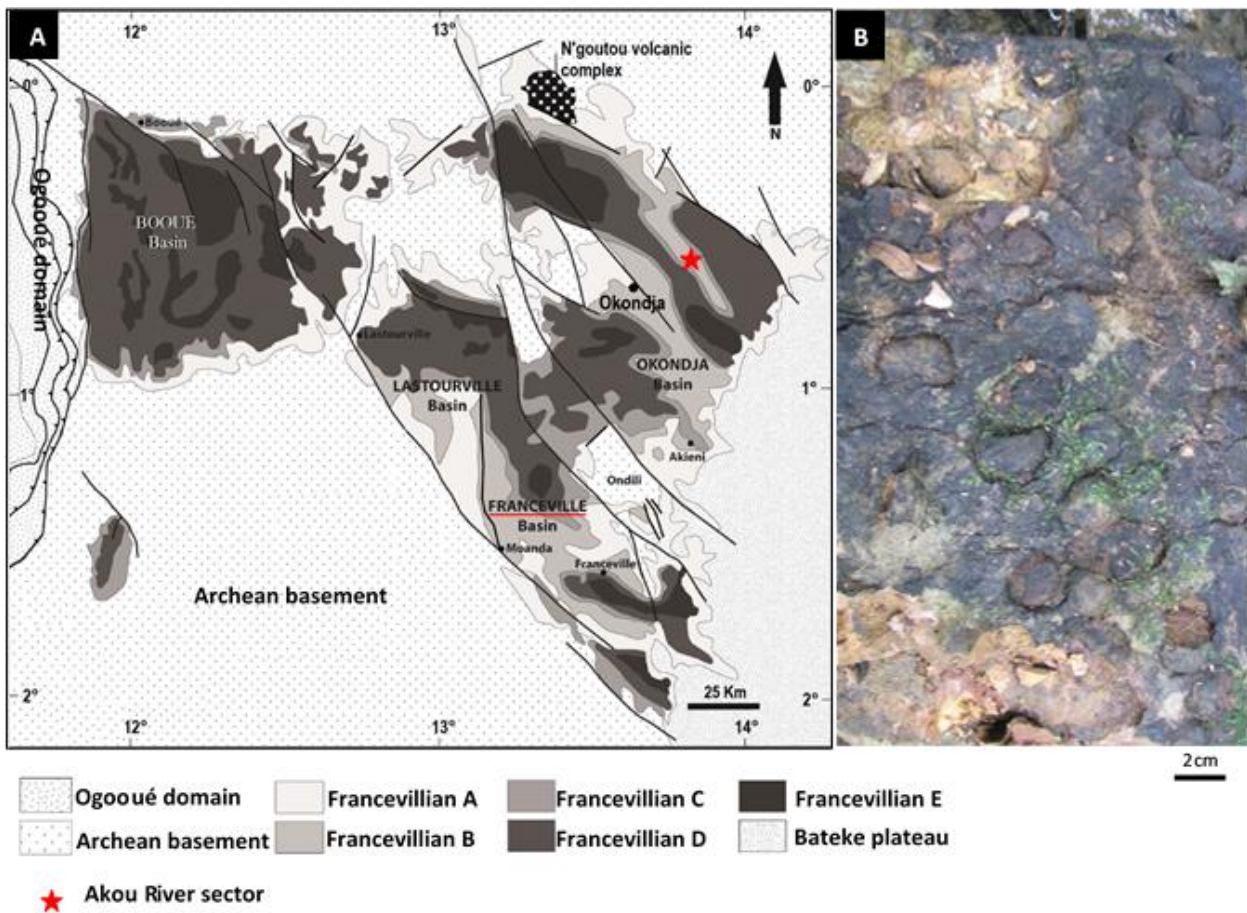


Figure S1: Geological map showing the context of fossiliferous Palaeoproterozoic rocks in Gabon. (A) Archean basement is overlain by four sedimentary basins, including the Okondja Basin which contains the Akou nodules reported here. (B) View of a bedding plane of the fossil level in the field, showing a dense packing of subspherical to elongate nodules.

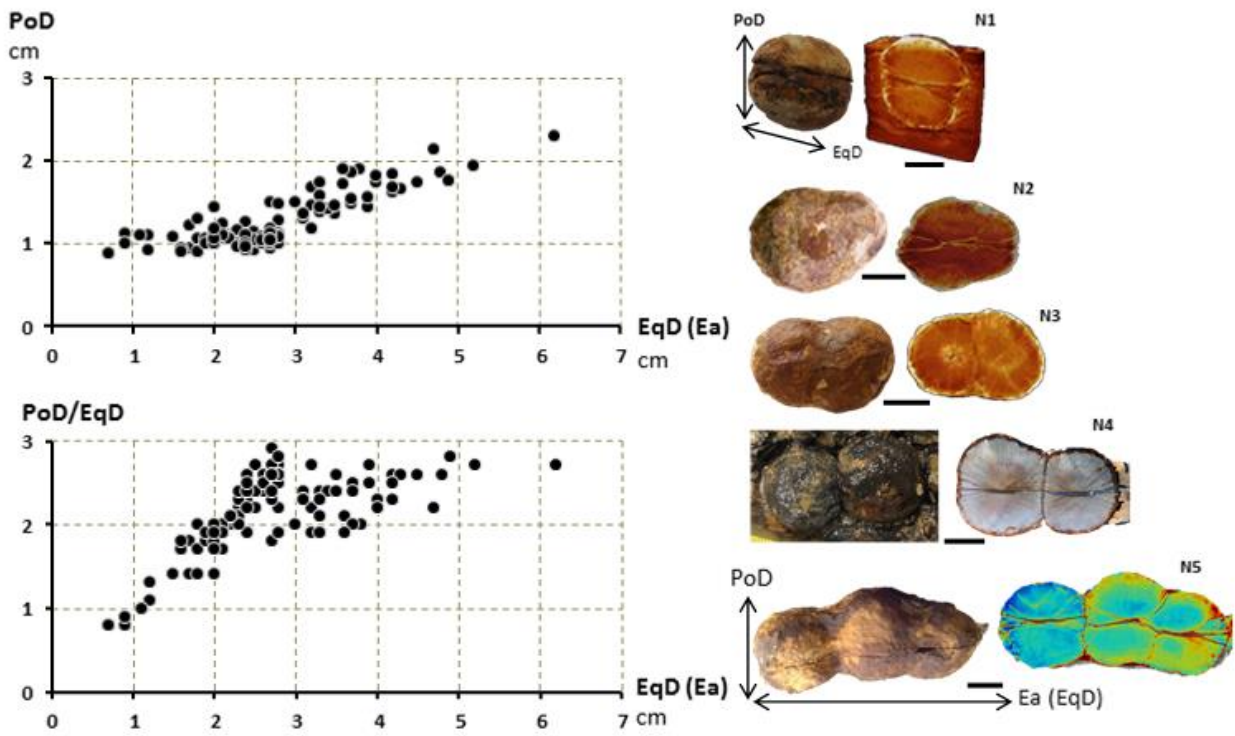


Figure S2: Graphs showing the range of polar diameter (PoD) and equatorial diameter (EqD) in the Akouemma nodules. These show a tendency for typical specimens to be ovoid (N1) and the elongated shapes showing a tendency towards lateral growth (N2-N5), “self-strangulation” (external furrow) and division (internal suture) (N3-N5). Ea: elongation axis) [8] modified. Scale bars: 1 cm.

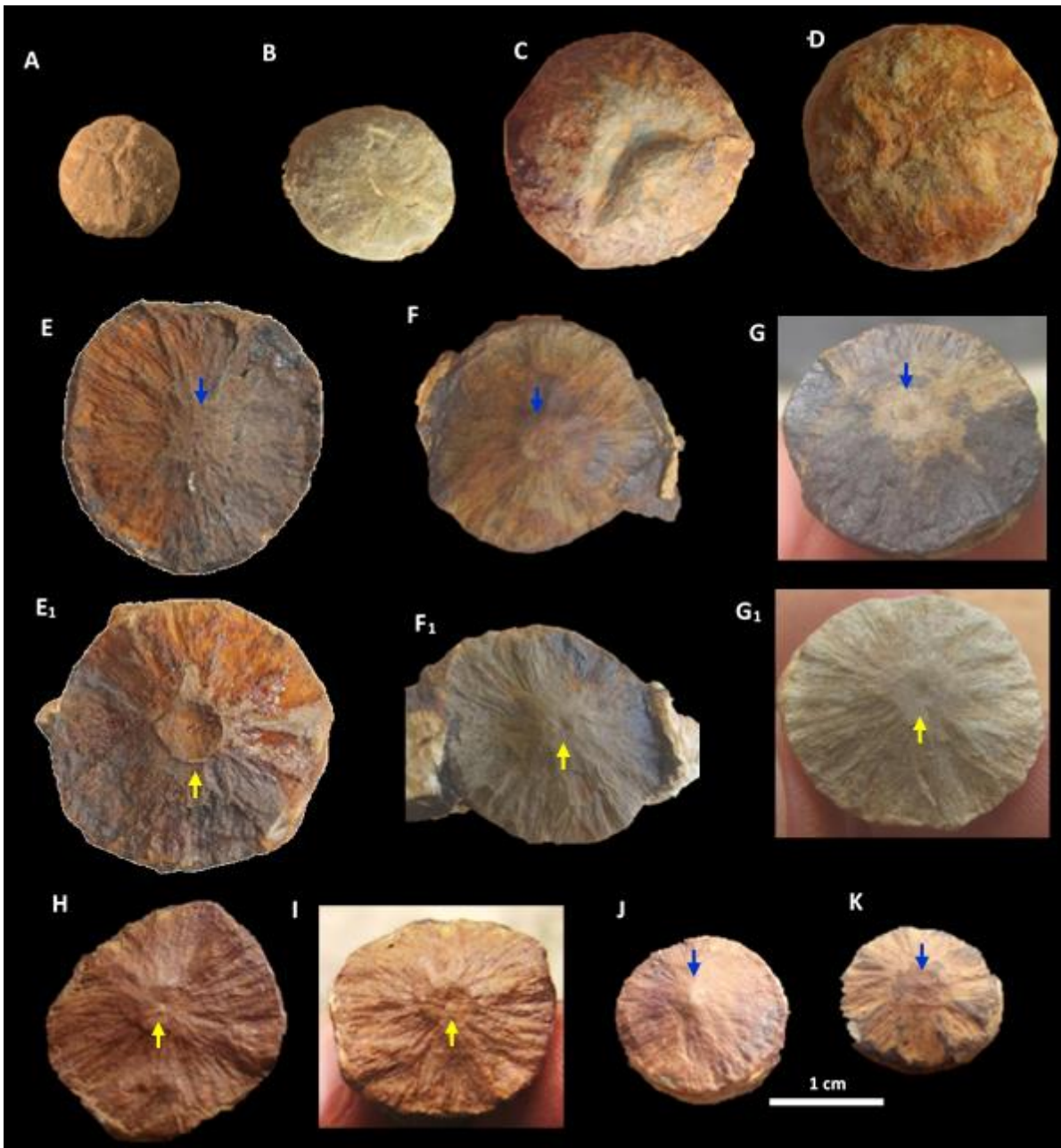


Figure S3: Morphology of the top of upper hemisphere and internal surface of hemispheres of ovoid forms nodule showing. (A-D) Views of the top hemispheres of four nodules of different sizes showing depressions around the top, dimples, lenticular shapes in relief. (E-G) Internal surface of upper hemispheres, showing radial sculpture and a central nipple-like feature (blue arrow). (E₁-G₁) Internal surface of lower hemispheres of same nodules, showing radial sculpture and a corresponding central depression (yellow arrow). The structures of the hemispheres G, G₁ of this nodule are well preserved compared to others. (H-K) Four hemispheres of four different nodules with nipple-like features and central depressions more or less well preserved.

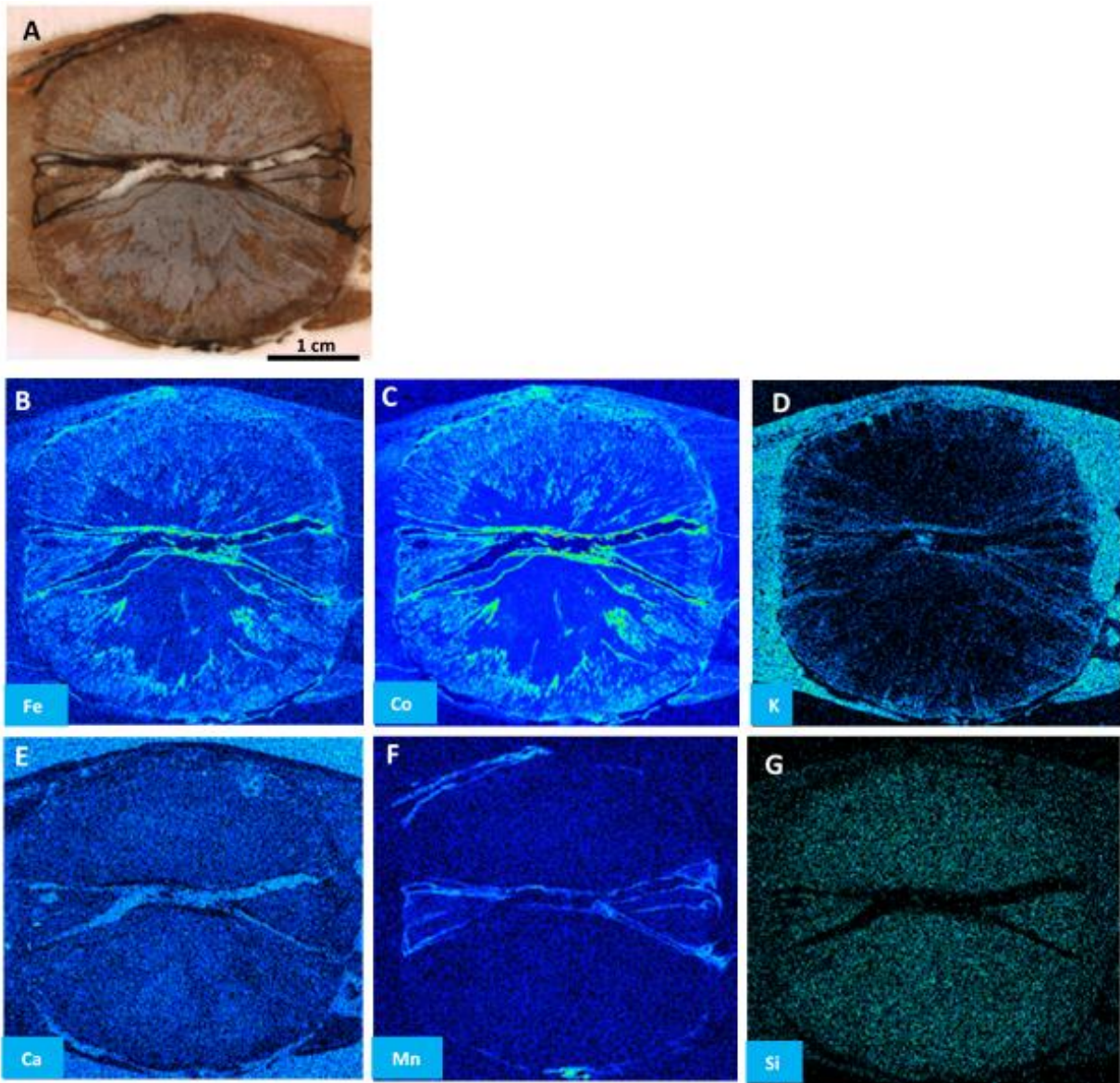


Figure S4: Images of distribution maps of chemical elements in a vertical axial section of *Akouemma* TS1 showing both hemispheres and the median disc; note the centrifugal fibro-radial system extending up into the upper hemisphere and down into the lower hemisphere. (A) BSE image. (B-G) Fe, Co, K, Ca, Mn, and Si distribution maps. The median disc, very fragile and susceptible to cracking, is highlighted by the Mn distribution map (F).

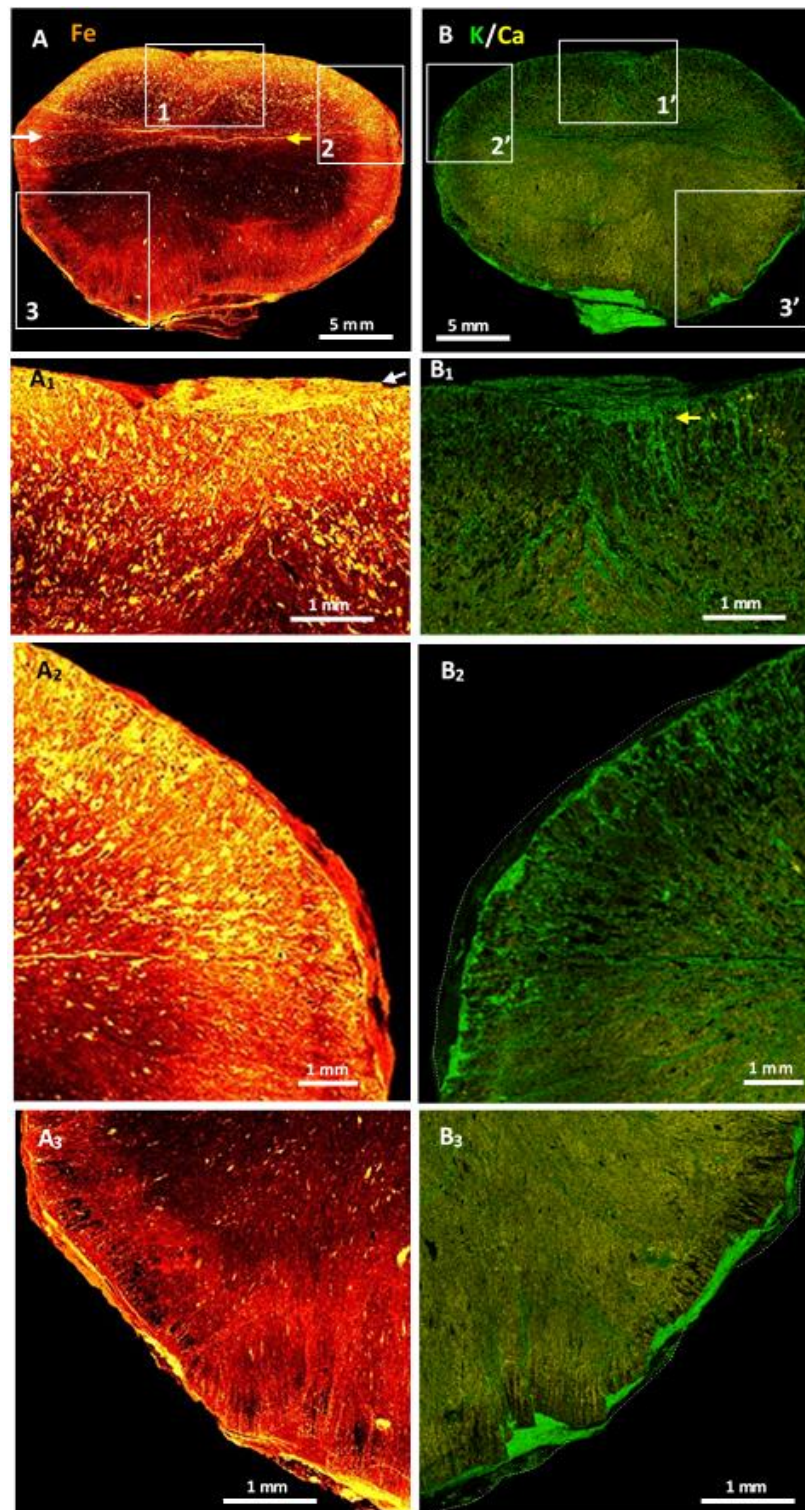


Figure S5: Particle-induced X-ray emission images of the distribution of iron, potassium and calcium in the Akou 16 nodule flattened in the upper hemisphere, highlighting its internal fibro-radial fabric and peripheral system. (A) Distribution of iron, which displays an internal radial system of fibres and particles from both sides of the median surface (yellow arrow); iron is more concentrated at the inner edge and forms a thin rim on the periphery. Note the tip of the median disc on the extreme left (white arrow). Boxes 1, 2, and 3 are shown in greater detail. (B) Distribution of potassium and calcium. Calcium has a more uniform internal distribution, whereas potassium is present in internal centrifugal fibres on either side of the median surface and forms a border around the edge of the nodule. Boxes 1', 2', and 3' are shown in greater detail. (A₁) Detail of box 1 showing a high density of iron particles and a lenticular body on the periphery (white arrow). (B₁) Detail of box 1' in the same zone showing a well-marked

radial system and the peripheral position of the lenticular body; note the flattened potassium fibres that have fossilized the deformation under the lenticular body (yellow arrow). (A₂) Detail of box 2 showing a view of both the radial and peripheral systems; note the abundance of iron particles in the radial system and the repeated patterns in the peripheral system. (B₂) Detail of box 2' in the same zone showing the two systems; the iron ring (dark green) is separated from the nodule by a thin border of potassium. (A₃) Detail of box 3 showing the radial system of denser iron filaments (a few particles are shown) and the peripheral system. (B₃) Detail of box 3' highlighting the peripheral system of repeating patterns of potassium (green) and iron (dark green).

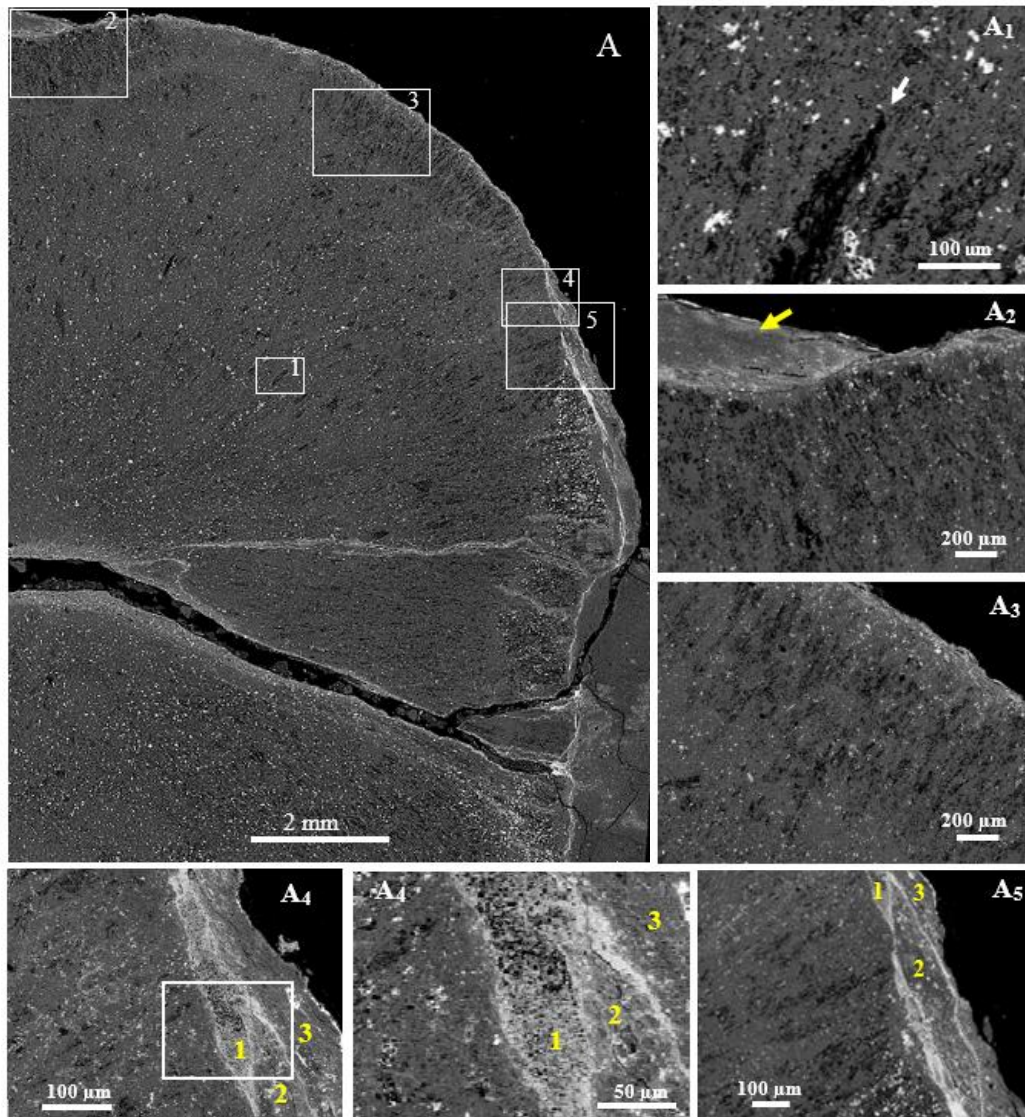


Figure S6: Scanning electron microscopic views of the internal and external aspects of an *Akouemma* nodule (Akou 3x021). (A) View of the upper hemisphere and the medial disc. The dark grey majority consists essentially of very fine silica. The light grey particles are iron, the grey particles are calcium (hardly visible), and the black areas are carbon-rich; note the radial arrangement of black lines of carbon from the centre of the medial disc to the rim of the upper hemisphere showing repeated patterns in the peripheral system similar to Figure S5A₂, A₃; iron is particularly concentrated on the edge and on the interfaces between the hemispheres and the middle disc. Images (A₁-A₈) correspond to boxes 1-8, respectively. (A₁) Magnification of the internal linear black carbon-rich area (white arrow). (A₂) Top of the upper hemisphere with a lenticular siliceous body in a depression; note the black linear pattern of carbon perpendicular to the rim. (A₃) The black pattern of carbon is densely distributed perpendicular to the rim. (A₄) View of lenticular bodies (1, 2, 3) parallel to the edge and the linear pattern of the carbon, which is always perpendicular to the rim. Note the superposition of the three lenticular bodies; the bottom one (1), in full, is 320 μm long and 40 μm thick. (A_{4a}) Details of three superimposed lenticular bodies (1, 2, 3); lenticular body (1) shows round patterns and carbon grains. (A₅) Another silicified lenticular body (2) at least 600 μm long and 95 μm thick; below, smaller iron-rich lenticular bodies and light grey iron particles can be seen in the nodule.

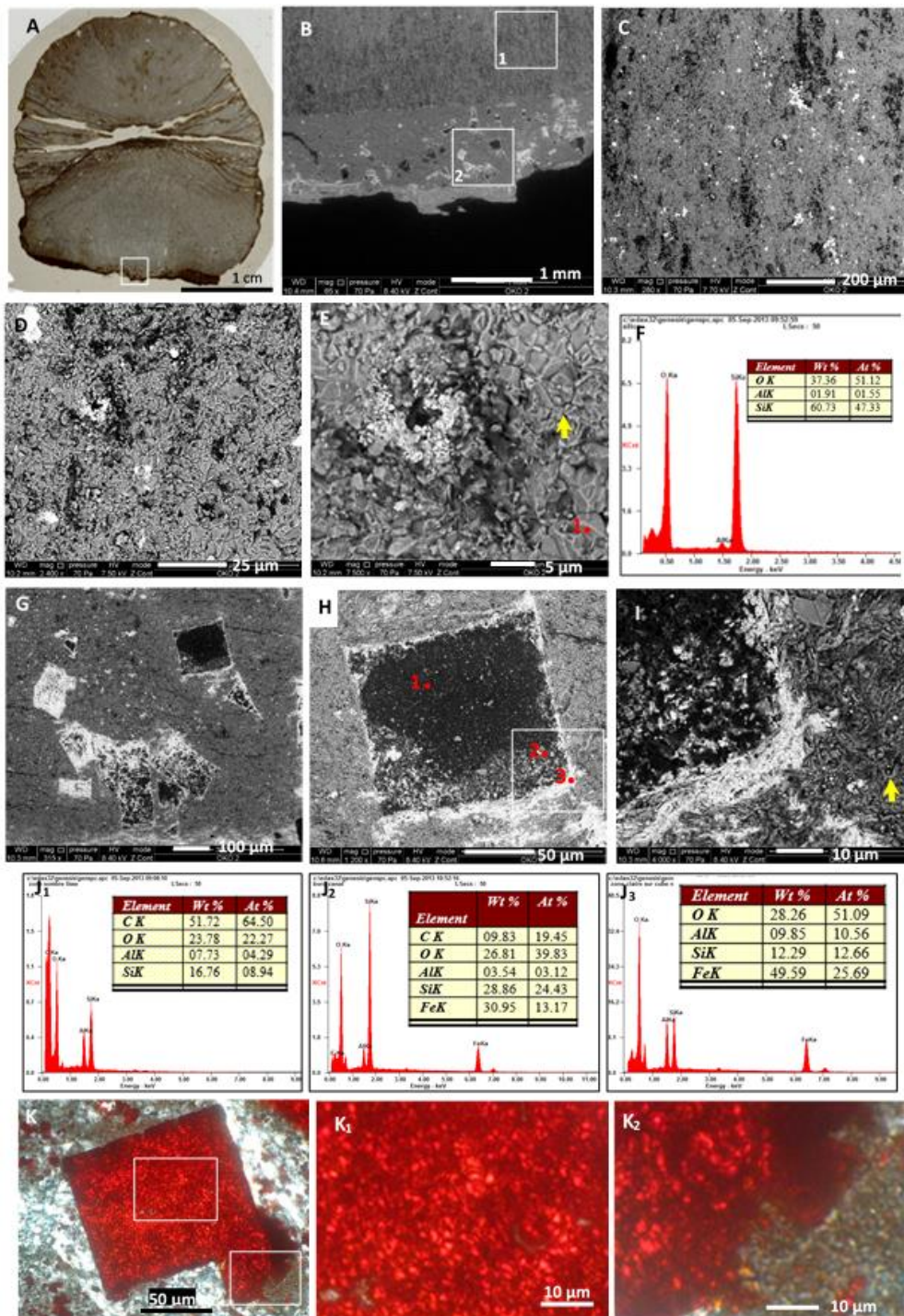


Figure S7: Some aspects of the internal structures of OKO 2. (A) Vertical section of OKO 2. The white frame on the edge indicates the area analysed. (B-I) SEM image showing in (B) the edge with two distinct zones: a radially structured zone with black traces of organic material aligned in the radial direction (Box 1) and a zone containing black and grey cubes with organic carbon and iron oxides (Box 2); the limit between the two zones is clear. (C) Detail of Box 1 showing clearly the traces of organic carbon in the radial direction and grains of iron oxide in the siliceous mass. (D) Micro-quartz siliceous background of box 1, showing in detail in (E) microcrystals of quartz approximately 2 μm in size. Analysis of point 1 indicates in (F) traces of Al in the silica. (G) Detail of Box 2 showing black organic carbon-rich cubes and light grey zones of iron oxide in a non-radial siliceous mass. (H) Detail of an organic carbon cube delimited by iron oxides. (I) Detail of the white box of (H) showing an edge of the cube in a siliceous mass with interlaced filaments (yellow arrow). The analyses of points 1, 2, and 3 are represented

in (J₁), (J₂) and (J₃). (K) "Cube" with red particles in the siliceous mass; note the net limit of the edges (AKOU 14 crossed nicols). (K₁) Magnified image of box 1 of the cube centre. (K₂) Magnified image of box 2 of the degraded border, revealing yellow-orange to greenish granules.

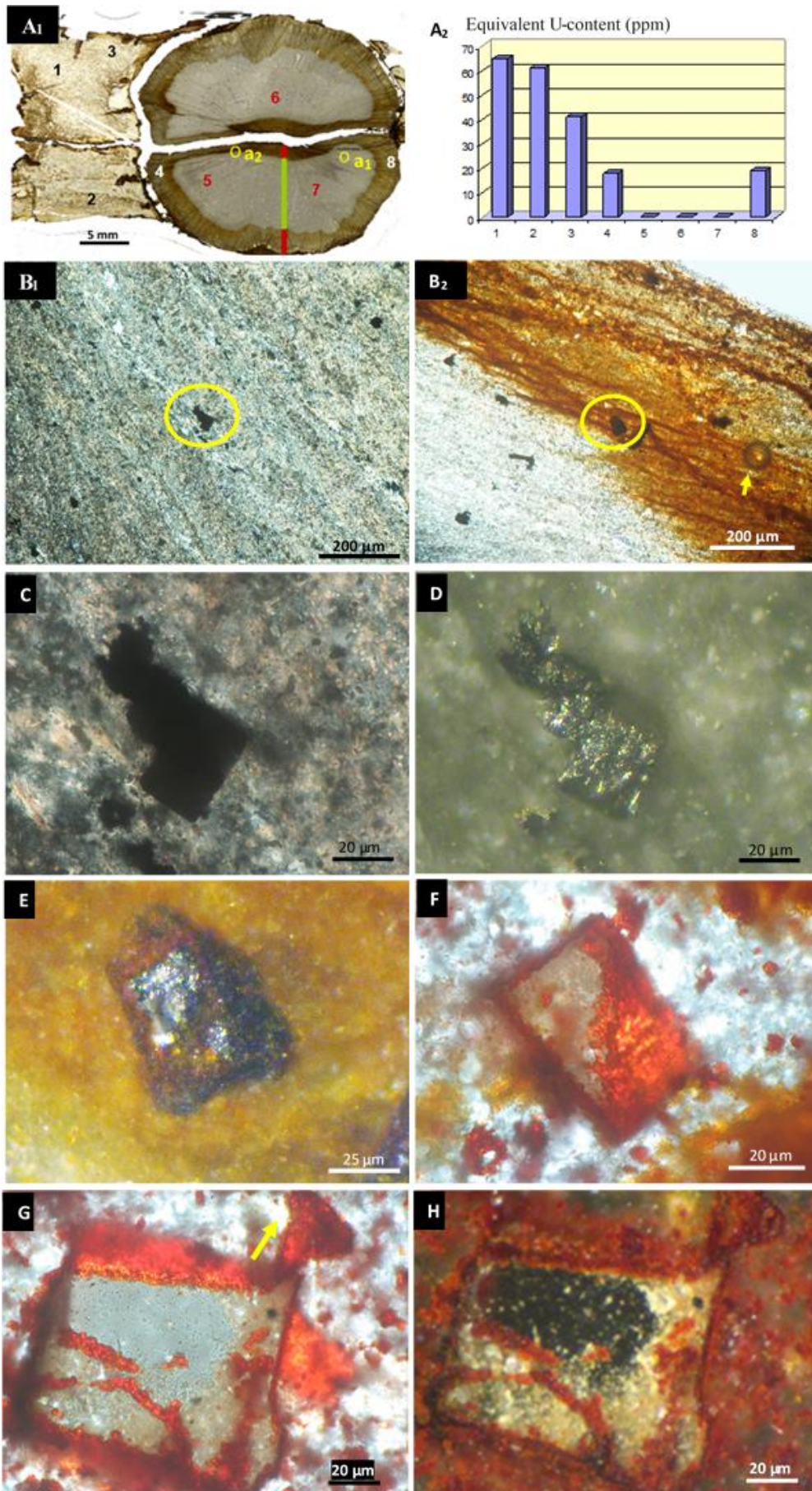


Figure S8: Radioactivity in AKOU 15 nodule and examples of pyrite and bricks with siliceous walls within the nodules. (A₁) Vertical section of AKOU 15 nodule with the gangue showing dark staining of the altered median

zone and the altered inner rim (0.2 mm wide); points 1 to 8 are analysis points of radioactivity. (A₂) Equivalent U-content (ppm) of points 1 to 8. (B₁) Thin section showing an unaltered internal zone with clay “channels” associated with opaque pyrite crystals, (circle a₁ in A₁, AKOU 15, crossed nicols). (B₂) Thin section showing an oxidized inner edge region with opaque crystals of pyrite and iron oxide; note the presence of an oblong shape with a pointed tip (white arrow) (circle a₂ in A₁, AKOU 15, crossed nicols). (C) Magnification of an opaque crystal of pyrite in the siliceous mass associated with clay minerals in ‘A’ (crossed nicols). (D) Magnification of the same crystal of unaltered pyrite; note the bristled surface of the crystal with particles in a vertical position (reflected light). (E) Magnification of the pyrite crystal in the oxidation process of ‘B’; note the surface bristling with light grey particles that are more or less aligned. (F) A brick with a siliceous wall showing a surface bristling with yellow-orange to red particles that are more or less aligned, as in figure (E) (AKOU 14, crossed nicols). (G) Another brick with a siliceous wall containing red particles that are aligned at the surface, note the “spreading” of the red particles out of the brick (yellow arrow) (AKOU 14, crossed nicols). (H) Same brick in reflected light showing black carbon particles in a siliceous wall delimited by red particles.

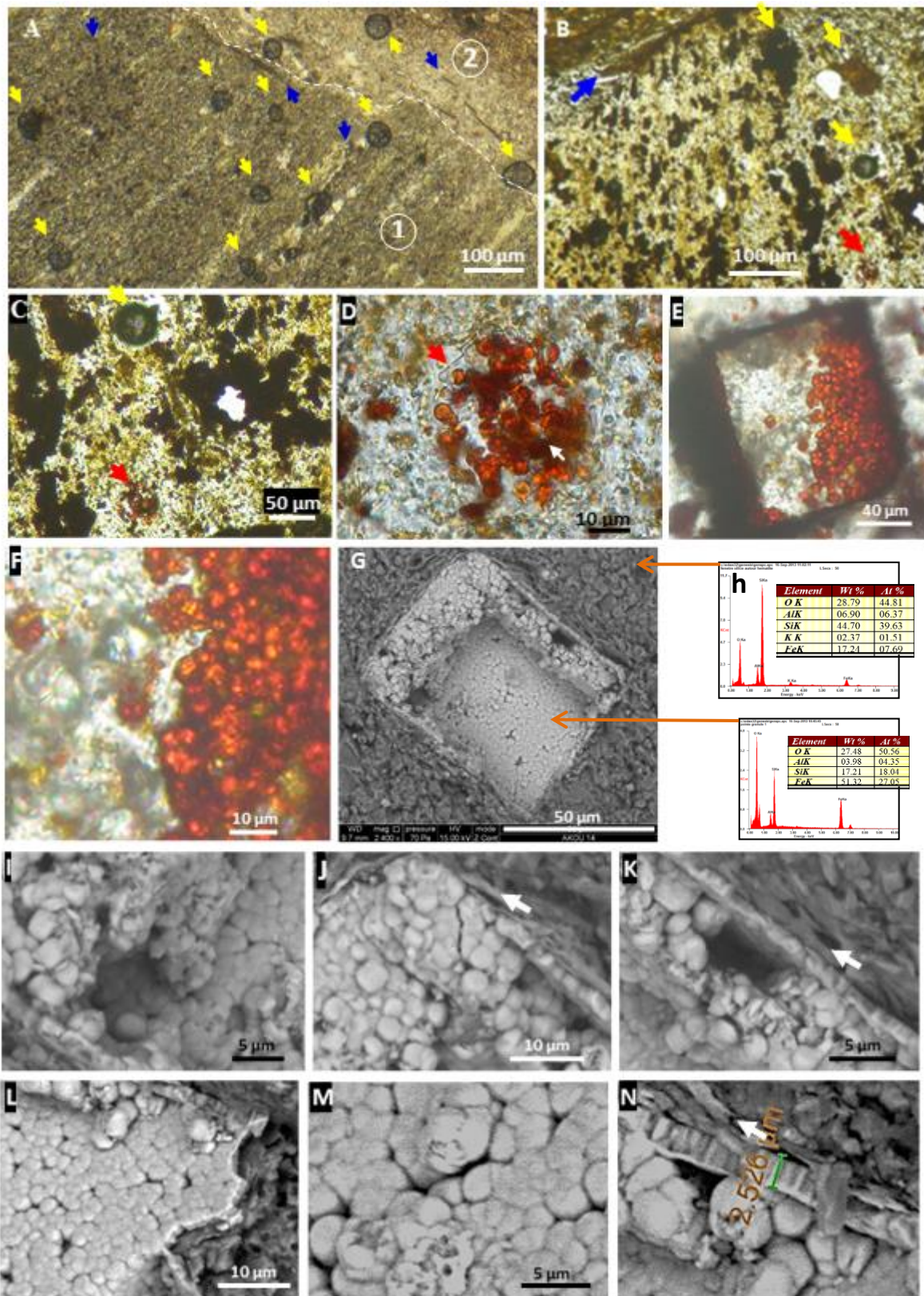


Figure S9: Oblong shapes, ferruginized spherules and particles contained in oblong forms, and ‘bricks’ in AKOU 14. (A-C) Microscopic views of oblong shapes along the transverse plane (yellow arrow); oblong-shaped bodies are dispersed in the specimen. The white dashed line separates the weathered edge (2) from the healthy part (1) (parallel nicols). Note the filaments disposed in the radial direction and intersecting this radial direction (blue arrows). (B-C) Among the oblong shapes, one contains red spherules (red arrow, parallel nicols). (D) Magnification of red spherules (cell-like) contained in a translucent silica wall and ending in a pointed tip (white arrow). (E) Microscopic

view of a silica 'brick' that contains and has on its surface greenish to red spherules; as in (D), the reddening of the spherules is not diffuse, suggesting ferruginous mineralization of these particles and spherules. (F) Magnification of greenish and red spherules on the surface of silica 'brick', some ones are decayed. (G) Scanning electron microscopic views of a 'brick' containing ferro-silico-aluminous spherules approximately 2-5 μm in size in the siliceous mass; note the regular arrangement of these particles. (H) SEM analysis of siliceous mass and spherules. (I-N) Detailed view of various aspects of the particles; note in (N) the 2.5- μm -thick ferro-siliceous wall lined on the inside by a thin ferruginous layer and the perpendicular disposition towards the exterior of rods of substantially the same size. (A-F: parallel nicols).

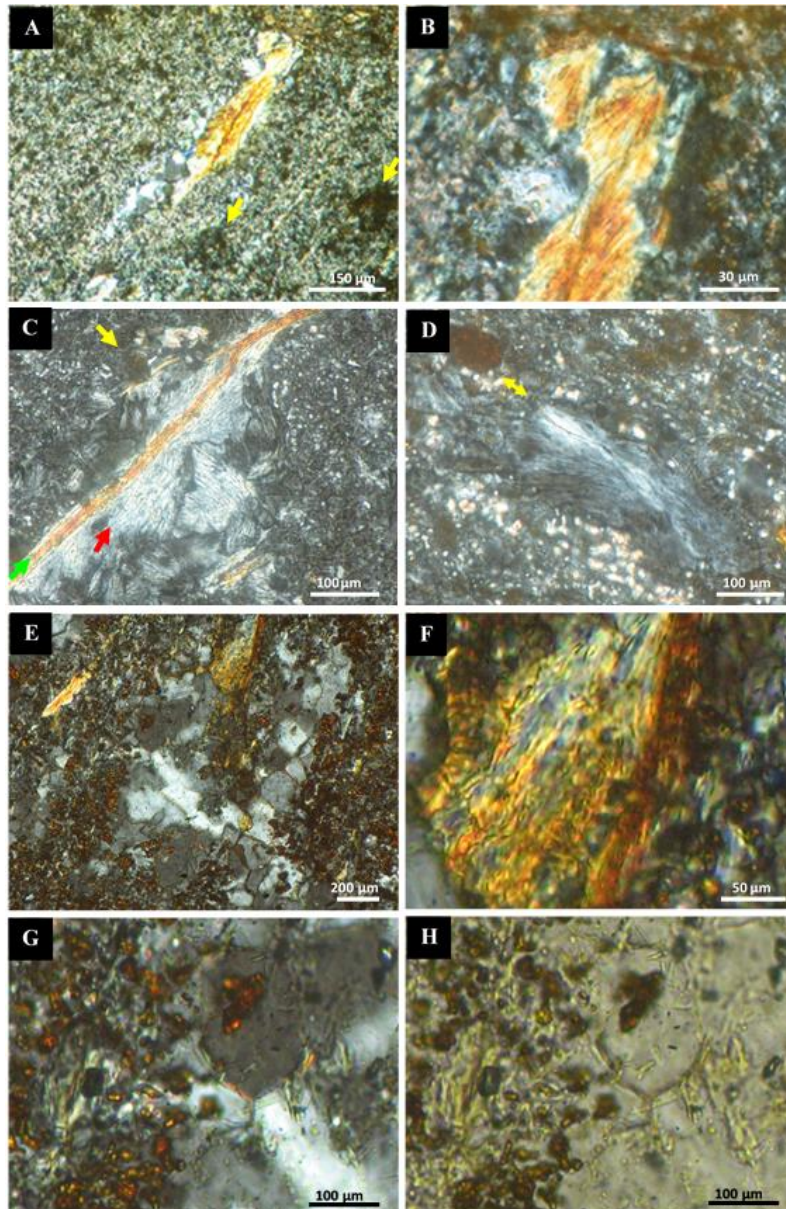


Figure S10: Various aspects of neof ormation clay minerals and other particles caught up in the micro-quartz crystals. (A) View of s yellow-orange elongated lepidocrocite similar to the silica lenticular bodies; note the alignment of dark oblong forms (yellow arrow) (Akou 16, crossed nicols). (B) Zoom of the lepidocrocite (high birefringence). (C) View of a yellow-orange filament of lepidocrocite $>500 \mu\text{m}$ in length (green arrow) and a neof ormation kaolinite (red arrow); note the dark grey oblong forms along the transverse plane (yellow arrow). (D) Neof ormation clay (kaolinite) that contains conserved elongated lenticular bodies aligned with a brown oblong form (organic matter, yellow arrow). (E) View of the yellow-orange lepidocrocite, brown oblong particles (organic matter), and lenticular body aligned in the same direction and embedded within the micro-quartz crystals. (F) Detailed view of the lenticular body; note the alignment of lepidocrocite fibres on the surface and the internal arrangement of black carbon particles. (G-H) Detailed view of clay minerals, brown oblong particles embedded within the micro-quartz crystals. (A-G: crossed nicols; H: parallel nicols).

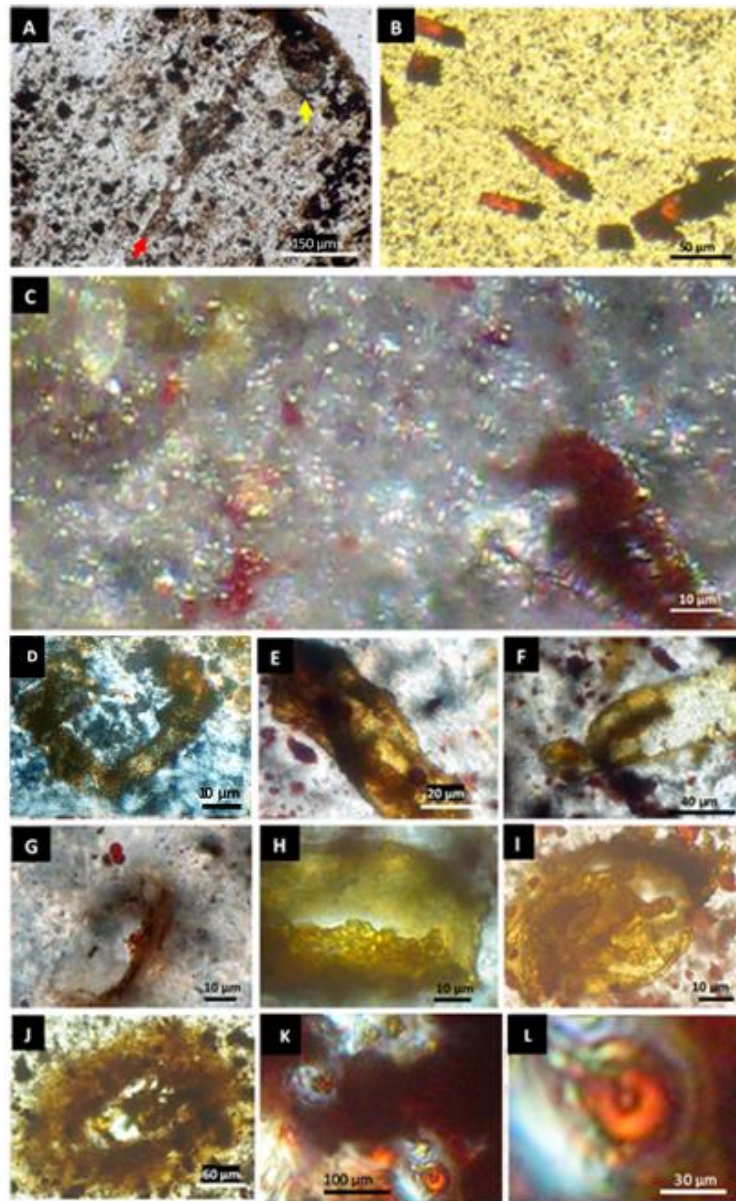


Figure S11: Linear, broken and decayed tubules, cell-like particles, and oblong shapes observed in the nodules. (A) Microscopic view of a linear tubule more than 5 mm in length in the radial direction (red arrow); note the presence of an oblong-shaped biomorph (yellow arrow). (B) Microscopic view of ferruginized broken tubules dispersed in the siliceous mass, suggesting fluidity prior to silicification. (C) Microscopic view of an organized decaying ‘multicellular’ structure with cell-like dispersion; this dispersion is limited (the detached ‘cells’ retain a certain alignment) in that it can only occur in a more or less viscous medium prior to silicification. (D-J) Various fragments of broken tubules, in decaying colored green to rust-brown likely remains mineralized of algae; note the granular walls. (K) Silico-ferruginous mass containing green and red oblong shapes well preserved. (L) Magnification of red oblong-shaped form with a pointed tip, note the net limit of the edge (C, K, L: crossed nicols; D: analysed crossed nicols, A-B, E-J: parallel nicols).

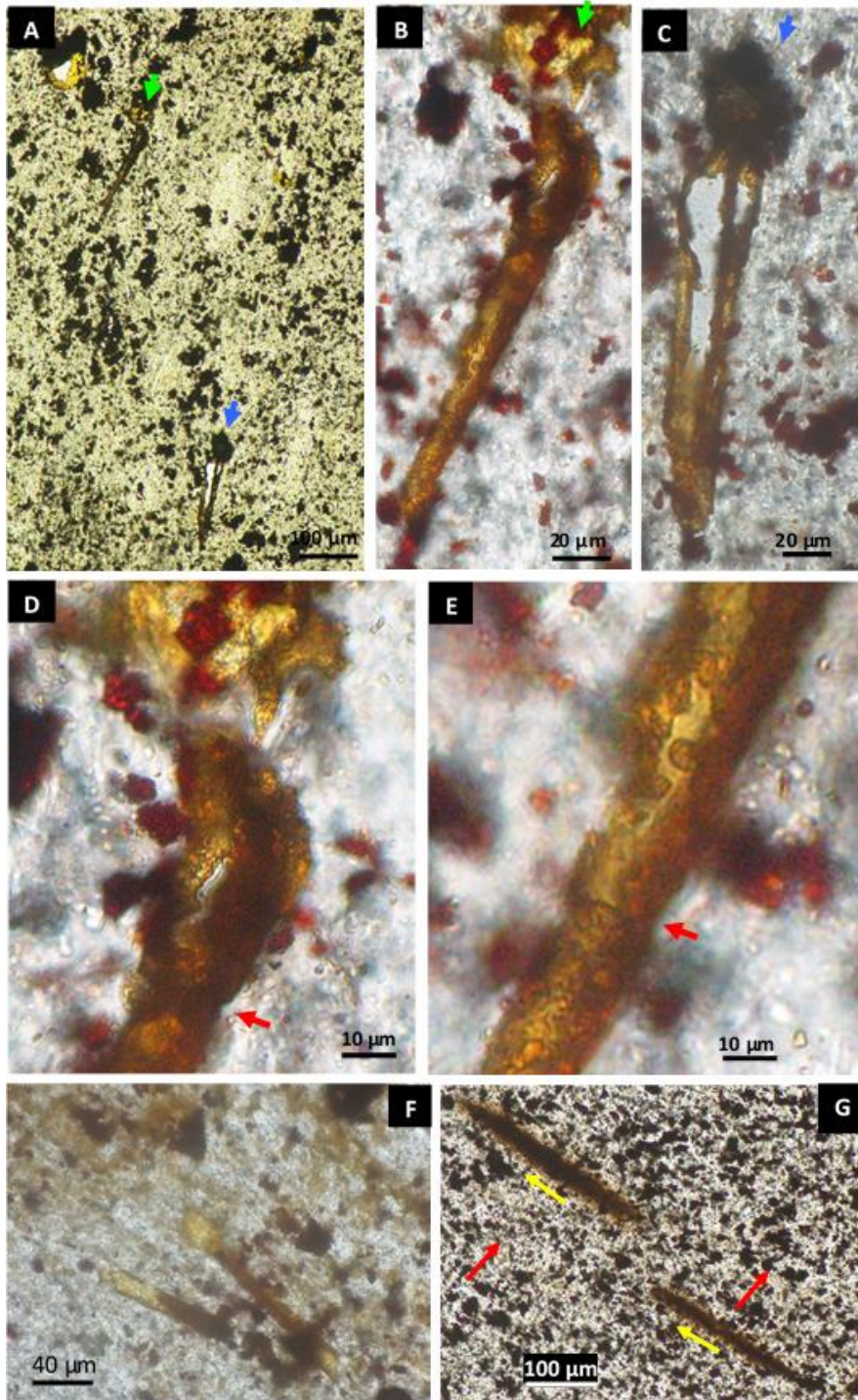


Figure S12: Other tubule features observed microscopically. (A) Views of two similar tubules in the siliceous mass associated with dark and yellow particles and areas. (B-C) Magnification of tubules showing rods, bulges and tufts probably of biologic origin (algae?). (D-E) Details of the tuft, bulges and the rod of the tubule (B); note the granulated wall and circular boundaries (red arrows), suggesting fitted-together parts. (F) Decaying parallel green filaments in the siliceous mass. (G) Elongated tubular shapes and dark particles in the siliceous mass; note two perpendicular directions (red and yellow arrows). (A-G: parallel nicols).

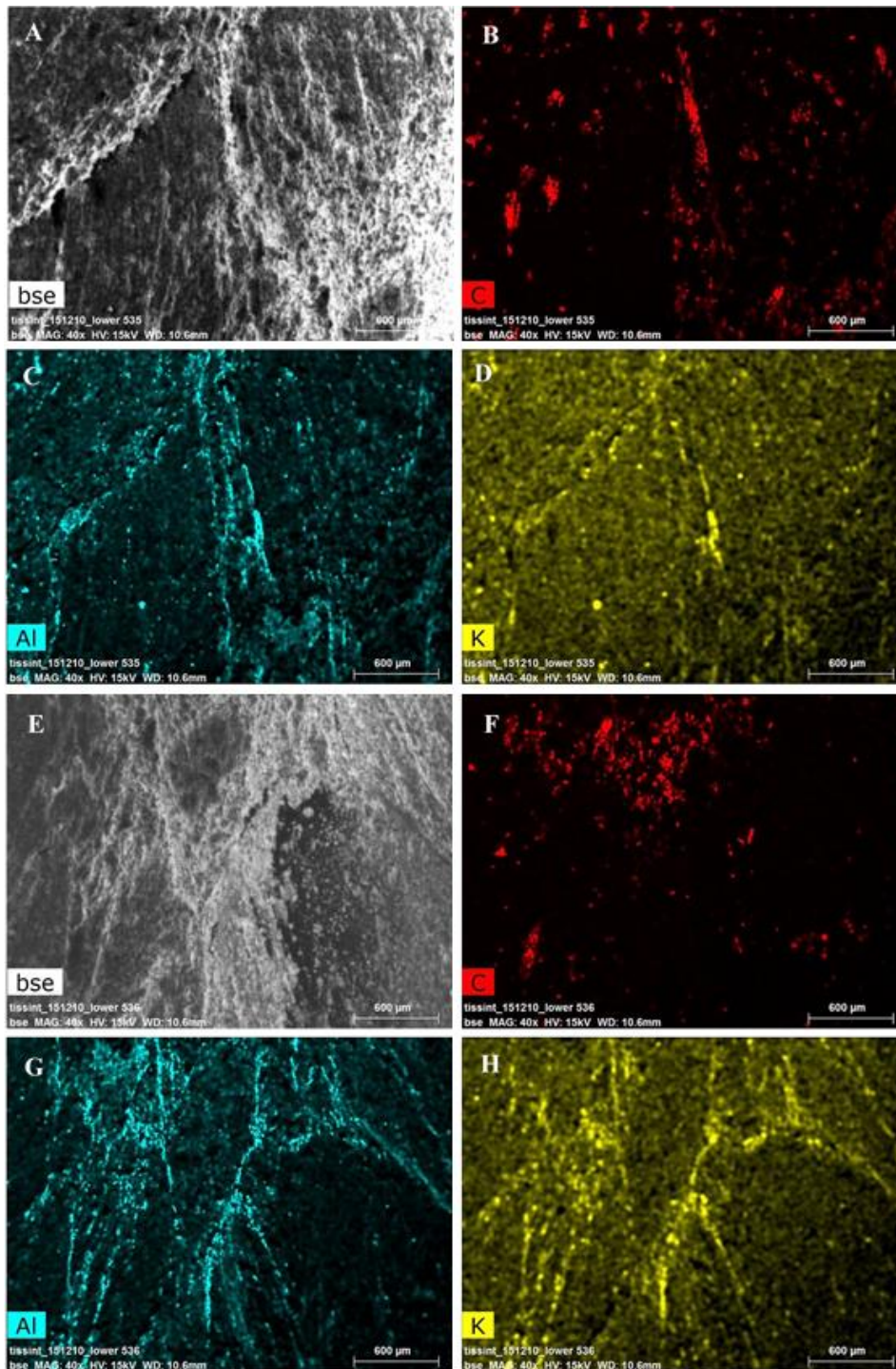


Figure S13: Internal fibro-radial fabric and chemical elements distribution map in *Akouemma* TS1. (A, E) BSE images showing the fibrous fabric. (B, F) Carbon distribution map. (C, G) Aluminum distribution map. (D, H) Potassium distribution map. Note the perfect superimposition of aluminum and potassium distribution maps with BSE images and the disposition of particles and carbon filaments more or less surimposable to aluminum and potassium.

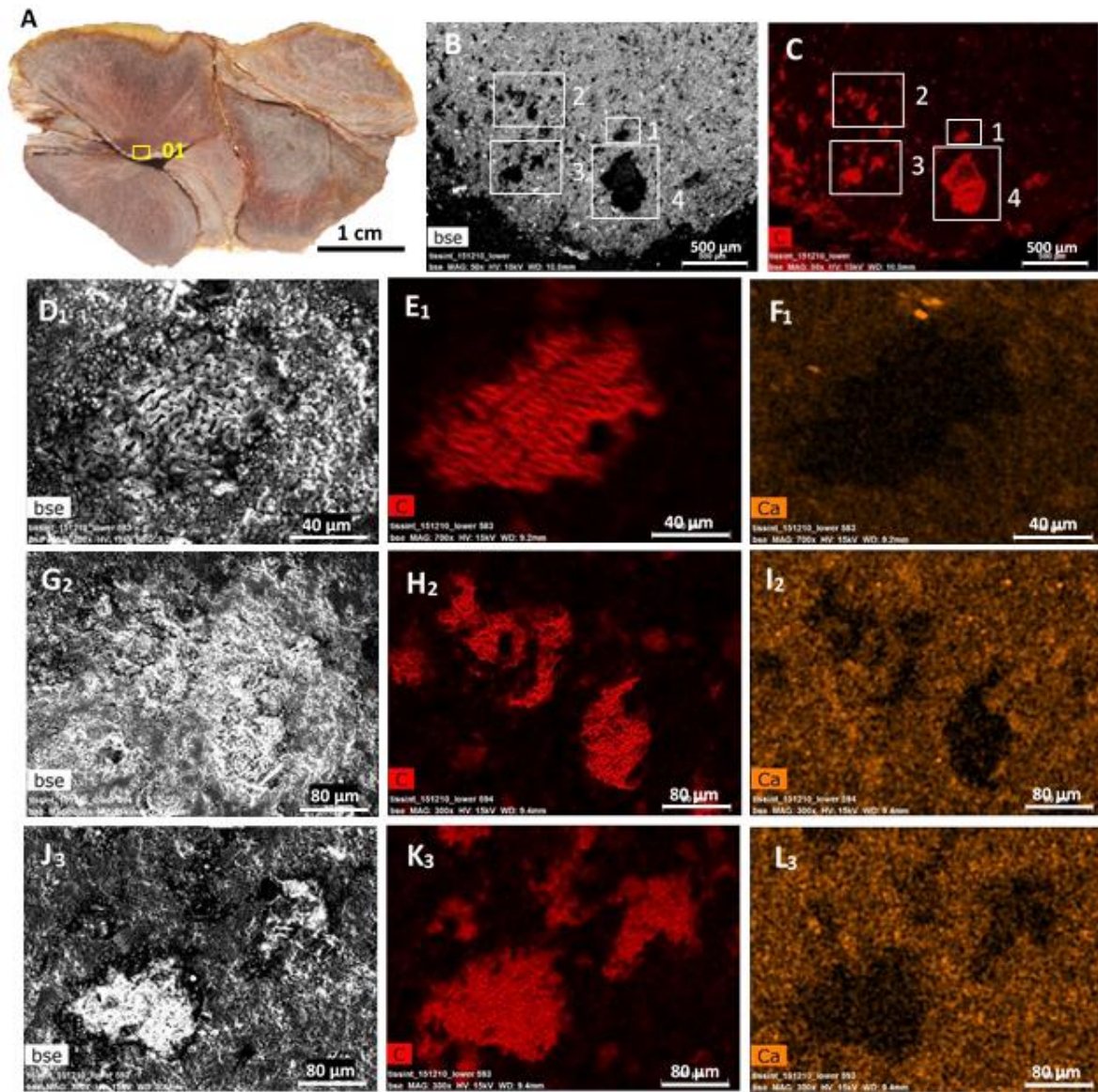


Figure S14: Internal structures of contiguous and deformed nodules of *Akouemma 2nd₁*. (A) Zone 1, cone of the upper hemisphere. (B) BSE image showing a centrifugal uniform radial system dotted with black spots distributed largely in the radial direction. (C) Carbon distribution map showing areas of concentration corresponding to the black spots in image (B). (D₁-F₁) Magnification of box 1. (D₁) BSE image showing a labyrinthine structure (E₁) Carbon distribution map showing a regular pattern structure. (F₁) Calcium distribution map showing grains a few microns in size around a calcium-free zone in the form of the carbon mass. (G₂-I₂) Magnification of box 2. (G₂) BSE image showing a highlighted xenomorphic structure. (H₂) Carbon distribution map showing vacuolar funnel-shaped bodies. (I₂) Calcium distribution map showing grains of a few microns around a calcium-free zone in the form of the carbon mass. (J₃-L₃) Magnification of box 3. (J₃) BSE image showing two highlighted encrusted bodies. (K₃) Carbon distribution map showing bodies with arrow-like shapes. (L₃) Calcium distribution map showing grains a few microns in size around a calcium-free zone in the form of the carbon mass.

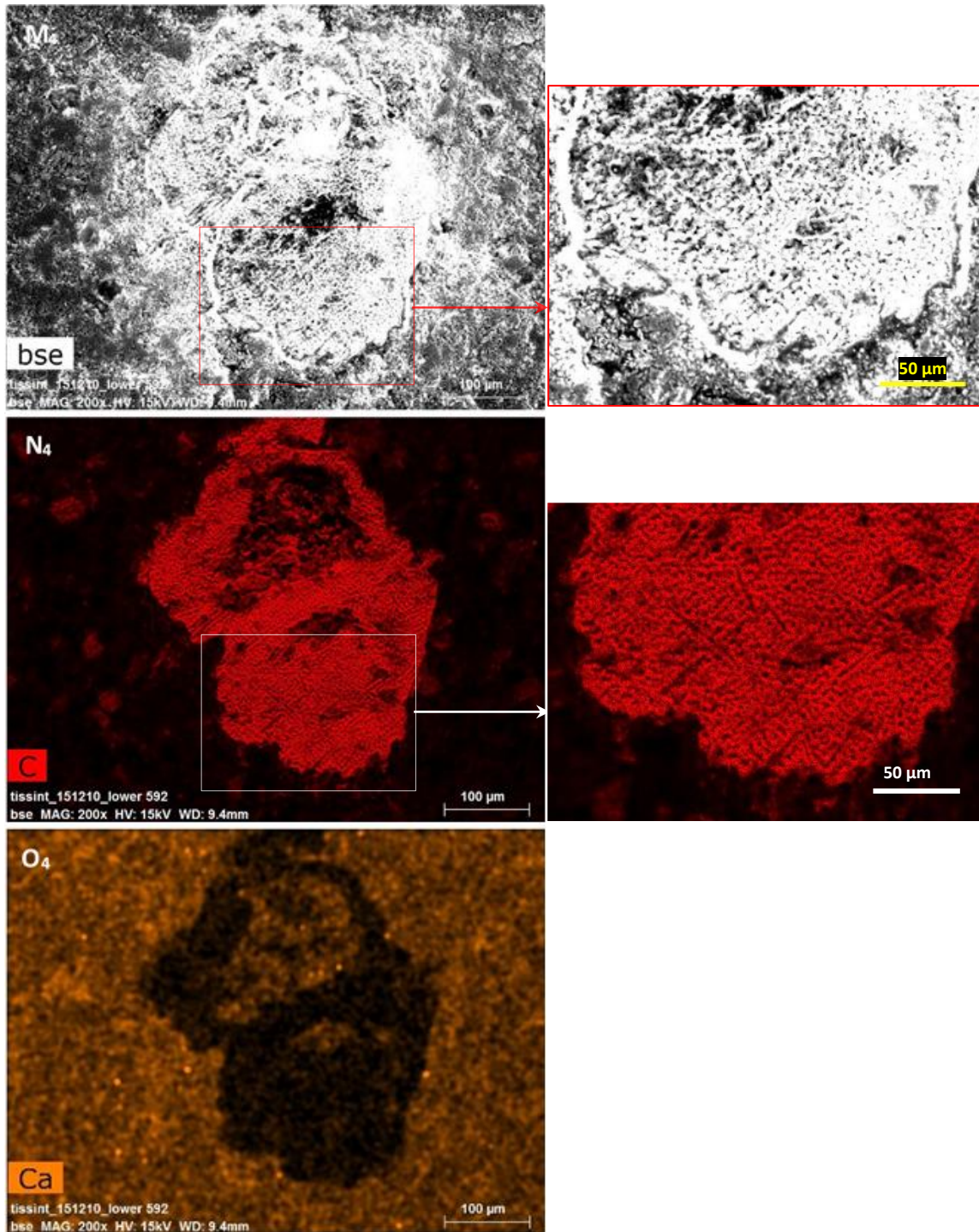


Figure S14: $bis_*(M_4-O_4)$ Magnification of box 4. (M_4) BSE image showing a highlighted circular shape. (N_4) Carbon distribution map showing an elongated xenomorphic mass with fine patterns. (O_4) Calcium distribution map showing grains a few microns in size around a calcium-free zone in the form of the carbon mass. All of the distribution maps of the chemical elements show the same configuration with respect to the carbon mass.

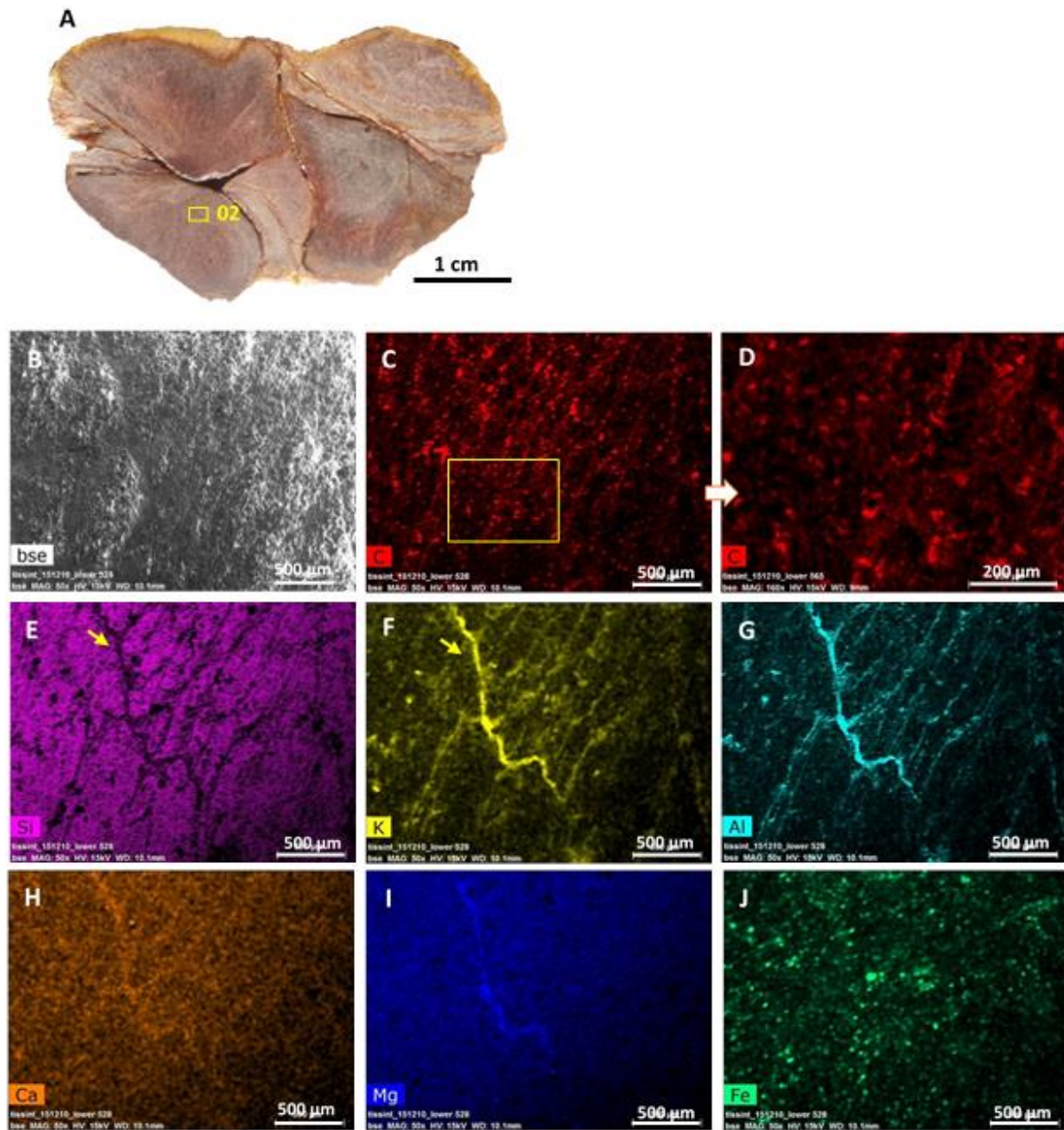


Figure S15: Internal structures of contiguous and deformed nodules of *Akouemma 2nd*. (A) Undeformed zone 2 of the lower hemisphere, presenting a fibrous structure in ‘tufts’ and ‘ramps’. The fibrous structure, which is barely visible on the BSE image (B), is highlighted by linear carbon fibres (C-D) in the radial direction. Dark traces in the silicon, and particularly aluminum and potassium images (E-G), highlight not only filaments that are superimposed on the carbon fibres but also the limits of the ramp structure. This structure is barely made visible by calcium (H). Magnesium (I) is just visible at the limits of a ramp. Iron (J) generally follows the orientation of the carbon fibres.

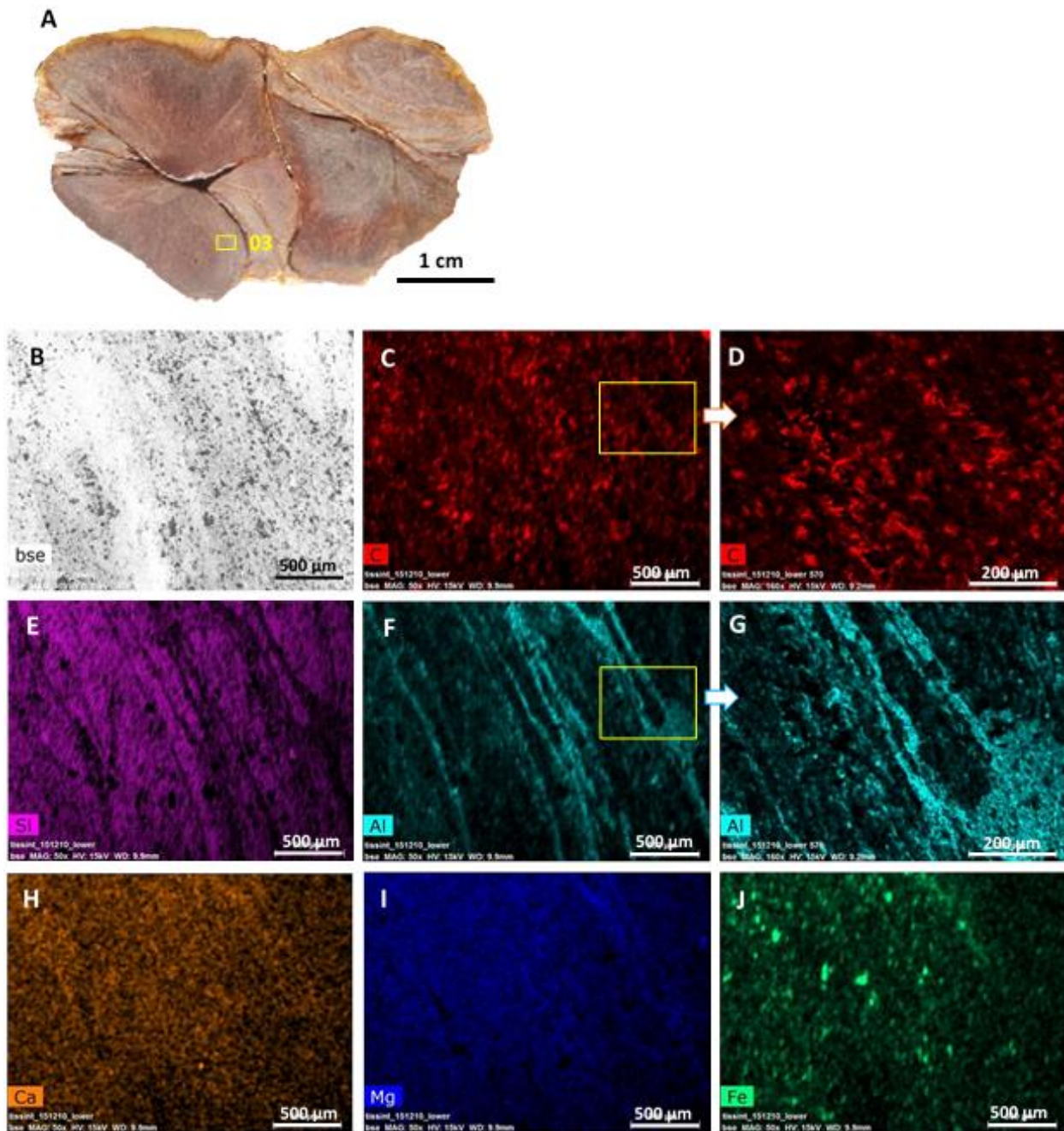


Figure S16: Internal structures of contiguous and deformed nodules of *Akouemma 2nd*. (A) Zone 3 is deformed, showing a flexed structure. (B) BSE image showing an entire zone bent in the orientation of carbon particles (C-D). The carbon particles are arranged in the same manner as the BSE image. (E-G) Curved linear structures are highlighted by dark traces on the siliceous mass (E) and by aluminum distribution maps (F-G) that present filaments and hollow tubules. (H-I) Calcium and magnesium distribution maps show a structure that is barely visible. (J) The iron particles are oriented in two directions; one is oriented along the bent structure, the other in an oblique direction.

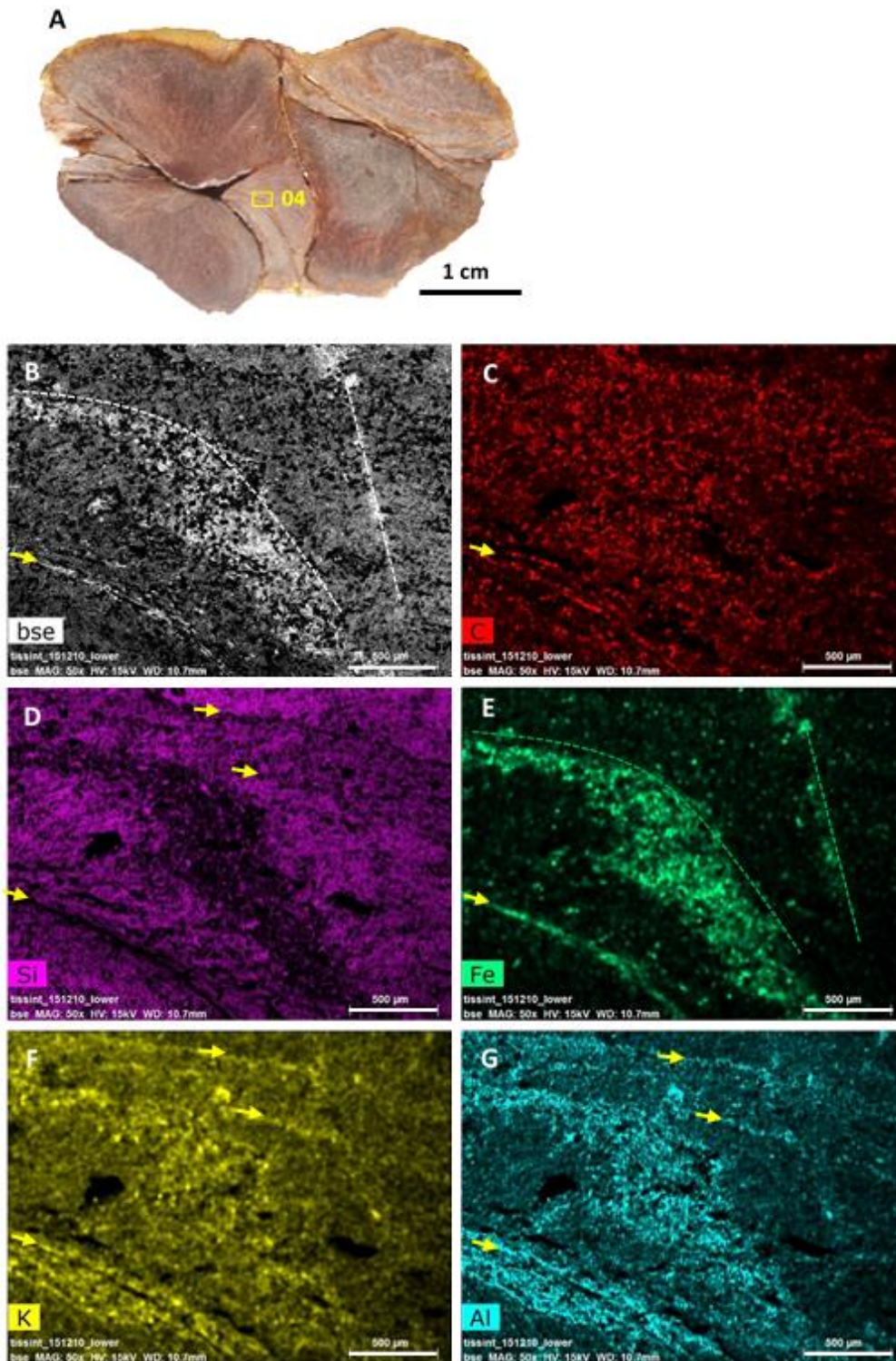


Figure S17: Internal structures of contiguous and deformed nodules of *Akouemma 2nd*. (A) Zone 4, compressed median disc. (B-G) All carbon, silicon, iron, potassium and aluminum distribution maps, including the BSE image, show the same deformation, with linear fibrous structures (filaments) at the lower left (yellow arrow), a turbulent zone with disorganized carbon particles above, and at least three planes with breaks in the slope (dotted lines). This suggests compression running from right to left.

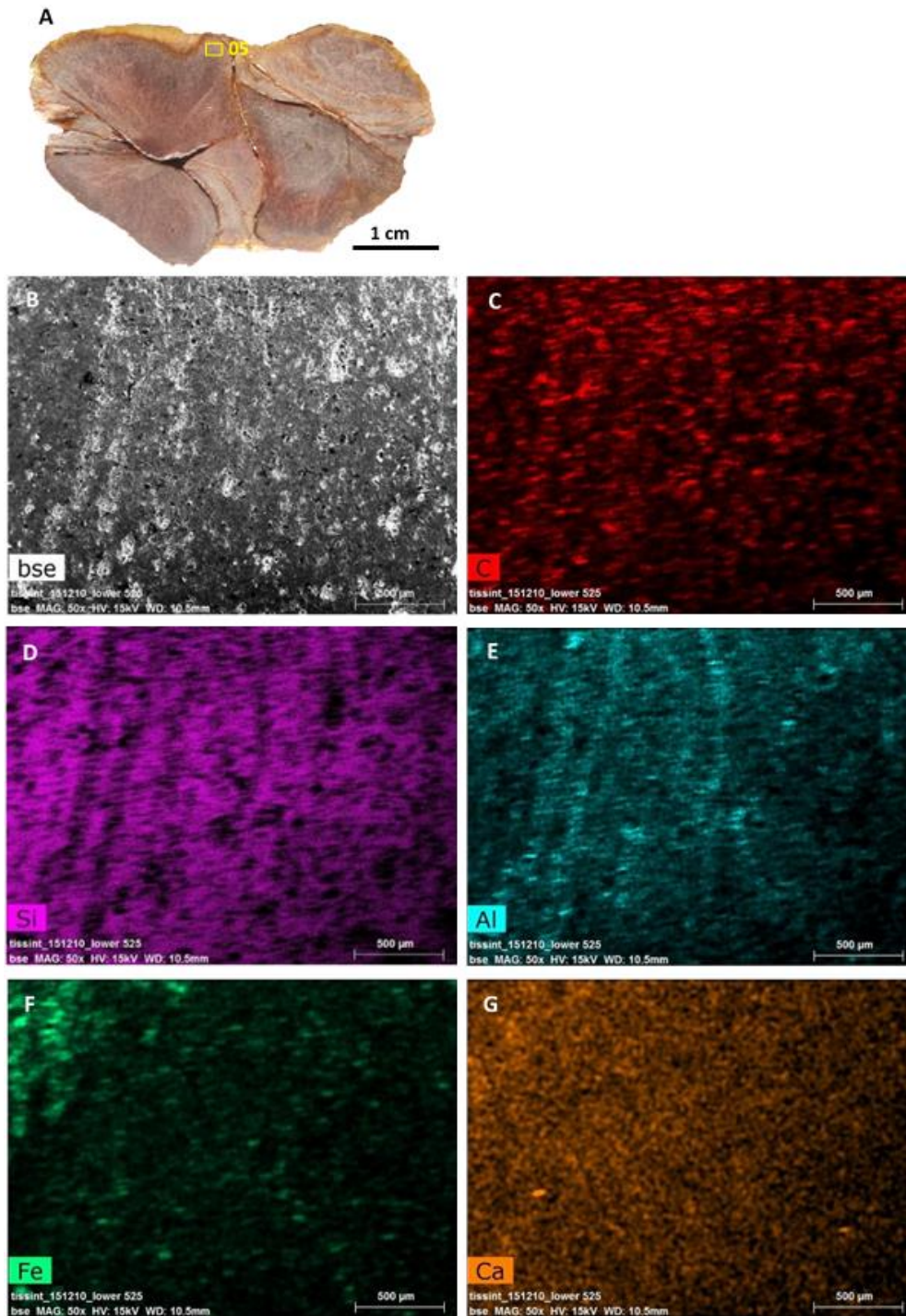


Figure S18: Internal structures of contiguous and deformed nodules of *Akouemma 2nd₁*. (A) Zone 5, which is compressed in the upper hemisphere. The compression zone 5 is accompanied by a reorganization of the internal structure. (B) BSE image showing discontinuous vertical structures. (C) The carbon distribution map shows vertically aligned and laterally stretched particles. (D) Dark vertical lines and lateral micro-shears in the siliceous mass. (E) Aluminum highlights straightened filaments that have been laterally micro-sheared off. (F-G) These deformations are very poorly (or not at all) recorded by iron and calcium. Note the similarities between the distributions shown in maps Al and C.

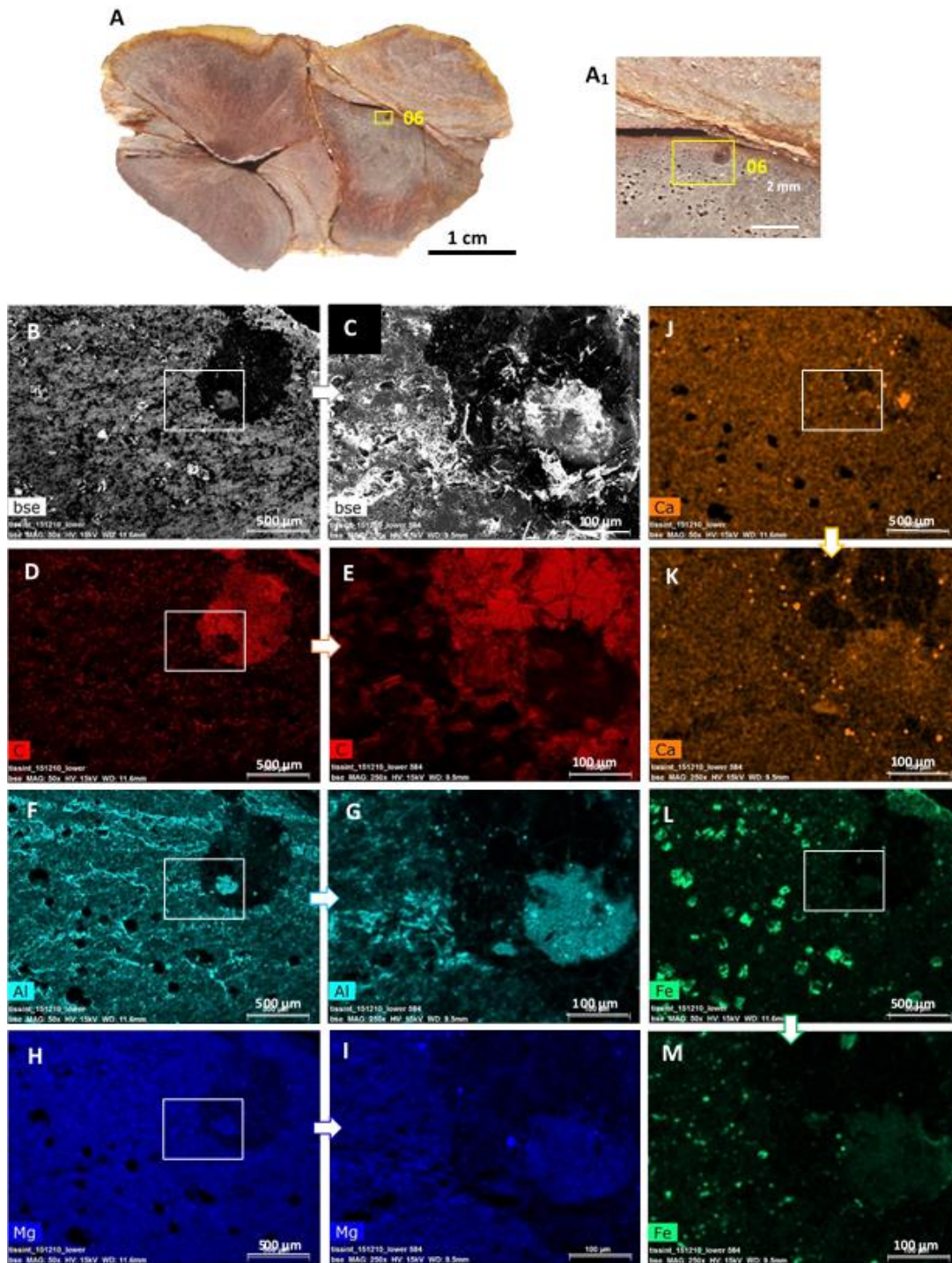


Figure S19: Internal structures of contiguous and deformed nodules of *Akouemma 2nd₂*. (A) Zone 6, undeformed cone of the lower hemisphere. (A₁) Macroscopic view of an oblong biomorph approximately 600 μm in diameter embedded in the nodule; note the surrounding scattered dissolution cavities. (B) Mottled grey BSE image showing black and white dots with no clear orientation and an oblong-shaped dark form within which there is a clearer, round zone. (C) Magnification of the box showing a clear zone with a pointed tip surrounded by dark and light zones. (D-E) Carbon distribution maps with magnified image (E) showing an oblong carbon form with a round dark zone at its tip. (F-G) Aluminum distribution maps with magnified image (G) showing no particular organization but displaying curving lines and scattered dark spots; aluminum seems to be present in zones with little or no carbon. (H-I) Magnesium distribution maps with magnified image (I) showing the same configuration as that of aluminum; the magnesium distribution is more homogeneous. (J-K) Calcium distribution maps showing a pervasive distribution of

calcium except in very carbon-rich areas and scattered dark spots. (L-M) Iron distribution maps showing concentrations in dispersed points (probably pyrite dissolution cavities) and secondary concentrations in less carbon-rich areas.

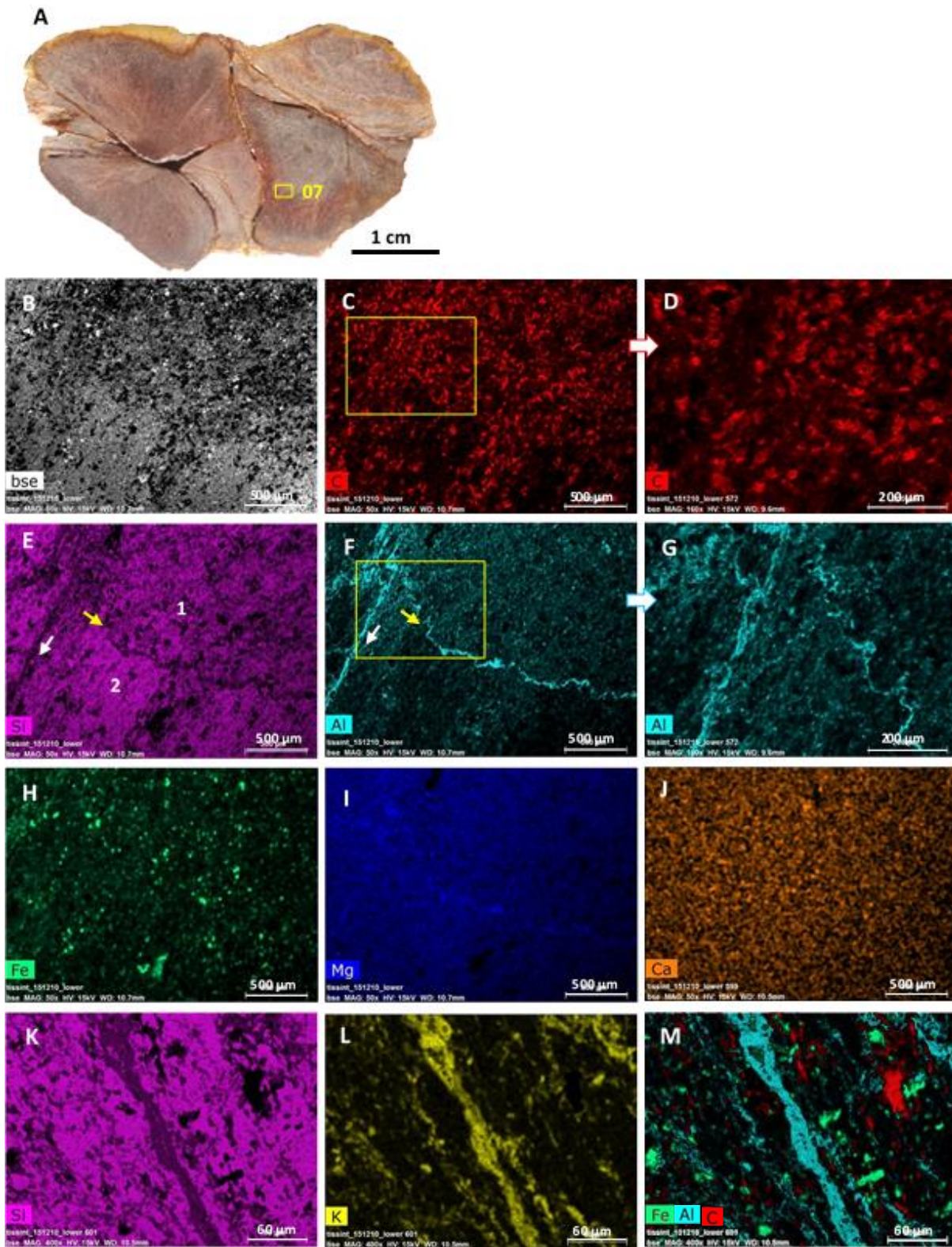


Figure S20: Internal structures of contiguous and deformed nodules of *Akouemma 2nd₂*. (A) Zone 7, undeformed lower hemisphere. (B) BSE image showing a marked oblique direction and a large number of dark particles in the upper half. (C-D) Carbon distribution maps with magnified image (D) showing the arrangement of particles in the same oblique direction as the BSE image. (E) Silicon distribution map showing a lateral line (yellow arrow) that seems to separate ramps 1 and 2 (ramp 1 covers ramp 2) and a linear structure extending in the radial direction (white arrow). (F-G) Aluminum distribution maps with magnified image (G), highlighting the limits of ramp 1 and the linear structure made up of juxtaposed patterns in the radial direction (clearly visible on (G)). (H) Iron distribution map showing the same configuration as the BSE image (B), with a higher particle density in the upper half of the map. (I) Magnesium distribution map; the linear structure extends in the radial direction, whereas the limit of the ramp is barely visible. (J) Calcium distribution map showing no orientation. (K-M) Distribution maps of silicon, potassium, aluminum, carbon and iron in thin section all show the same continuous or particulate linear structures in the radial direction (calcium, aluminum, carbon and iron) and discontinuous particulate structures that intersect in the radial direction (iron).

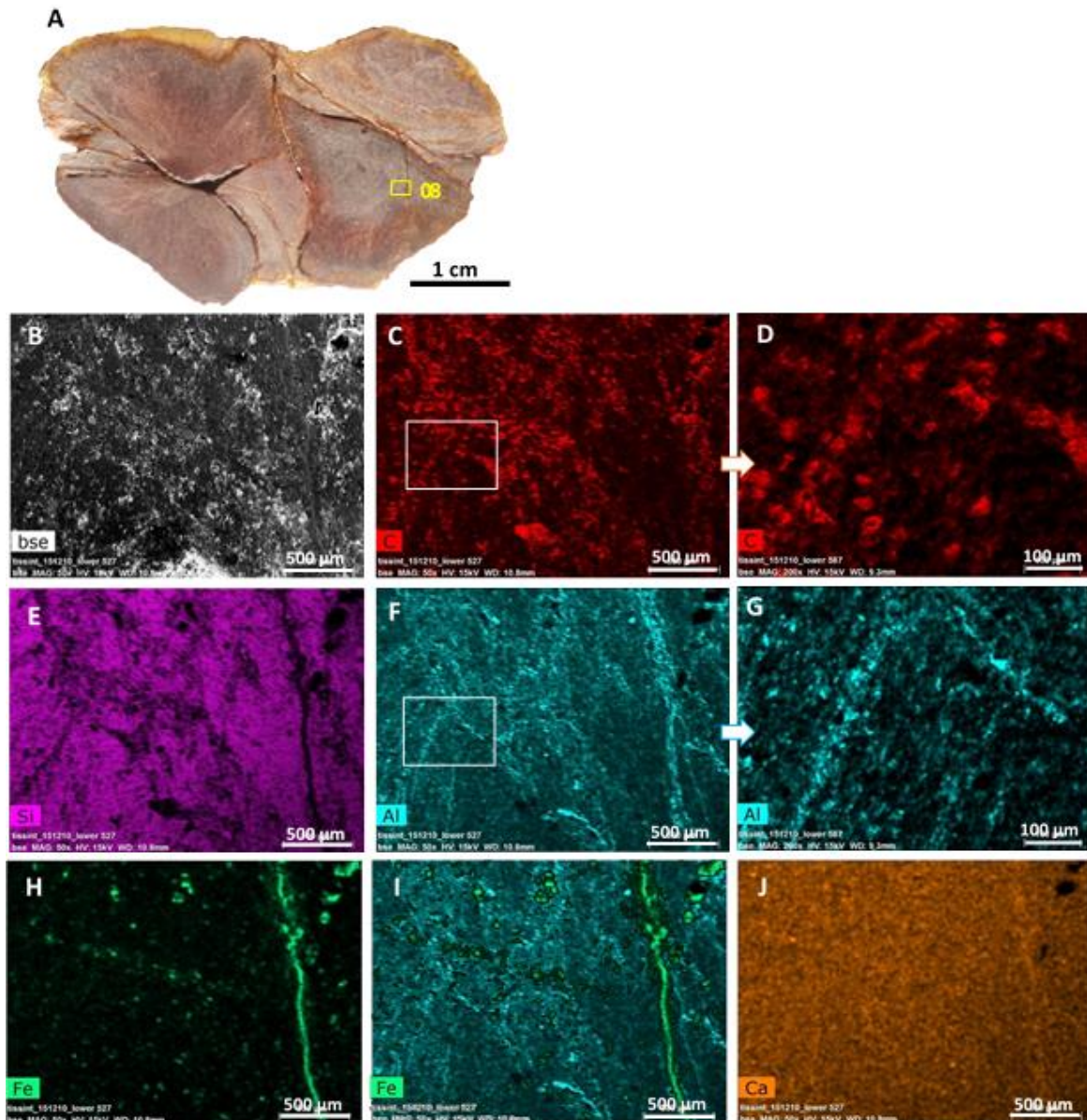


Figure S21: Internal structures of contiguous and deformed nodules of *Akouemma 2nd₂*. (A) Zone 8, partially destructured in the lower hemisphere. (B) BSE image showing curvilinear structures. (C-D) Carbon distribution maps with magnified image (D) showing a corrugated and heckled structure; particle size is approximately 30 μm . (E) Silicon distribution map showing gross curvilinear and linear structures. (F-G) Aluminum distribution maps with magnified image (G) showing these two structures in detail. Note the beautiful 'folded' structure associated with thin filaments in (G); this is superimposed on the carbon structure in (D). The thin filaments are parallel to each other and intersect the edges of the 'folded' structure; this zone appears to be degraded. (H) Iron distribution map showing a concentration of iron in the linear structure. (I) Superposed aluminum and iron distribution maps showing perfect juxtaposition of the two elements on the linear structure; the distribution of iron particles appears to be independent of the corrugations. (J) Calcium distribution map; the linear structure is only barely visible.

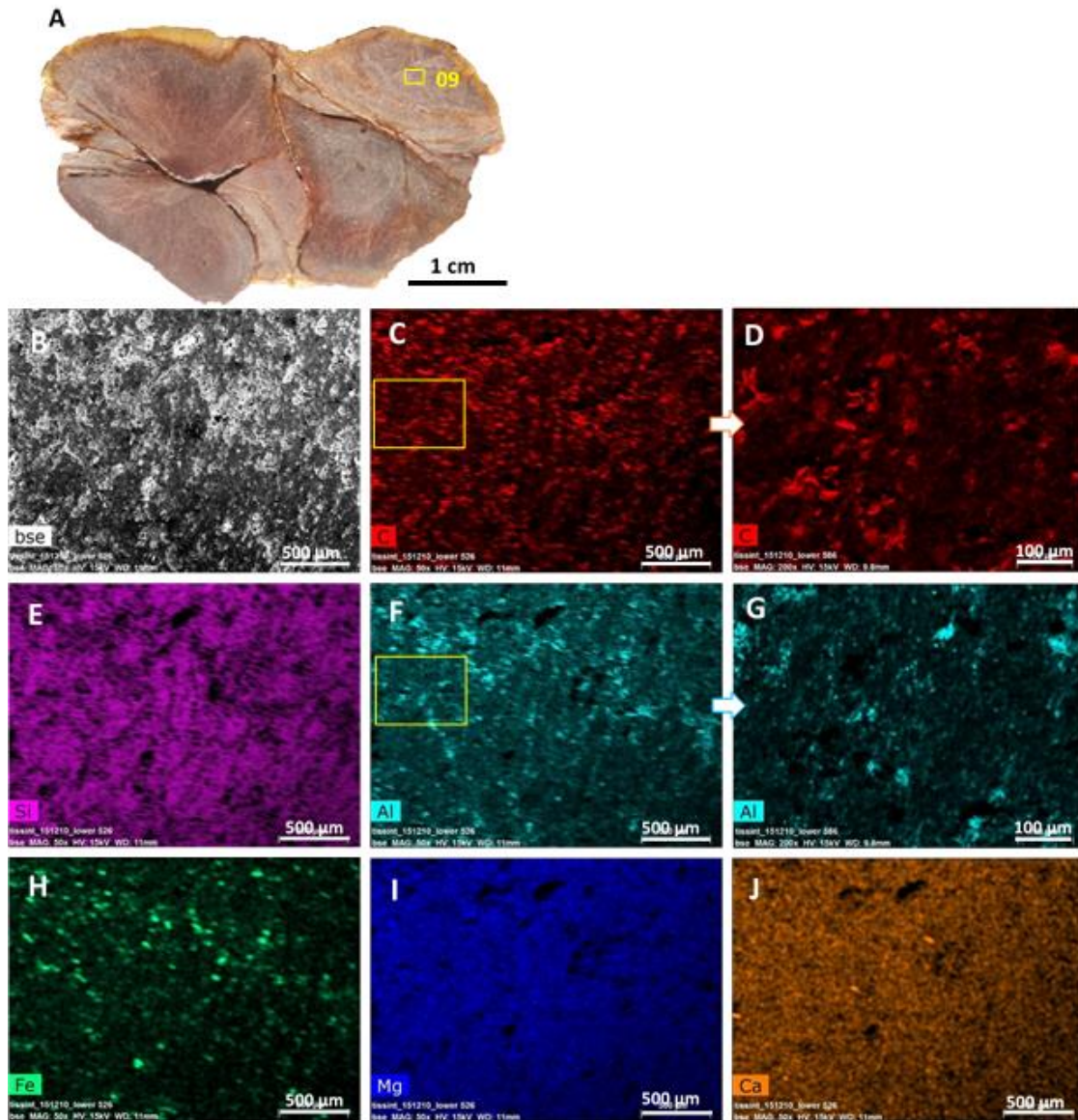


Figure S22: Internal structures of contiguous and deformed nodules in *Akouemma 2nd₂*. (A) Zone 9, undeformed. (B) BSE image showing an overall oblique orientation of linear structures in the lower half; the structures appear worn in the upper half. (C-D) Carbon distribution maps with magnified image (D) showing an overall particle orientation in the same oblique direction and details of the layout of curved carbon particles. (E) Silicon distribution map showing a complex structure involving transverse corrugated lines suggesting the edges of the flaps and finer lines of carbon particles in the oblique direction. (F-G) Aluminum distribution maps with the same configuration as that of silicon; transverse corrugated lines are discontinuous, suggesting disorganization. The magnified image (G) shows the overall oblique aspect of the structure; note the presence of large particles approximately 300 μm in size at the top of the image. (H) Iron distribution map that has the same general configuration as that of aluminum (F). (I-

J) Distribution maps of magnesium and calcium show a structure far less clearly but highlight large dark particles in an oblique direction.

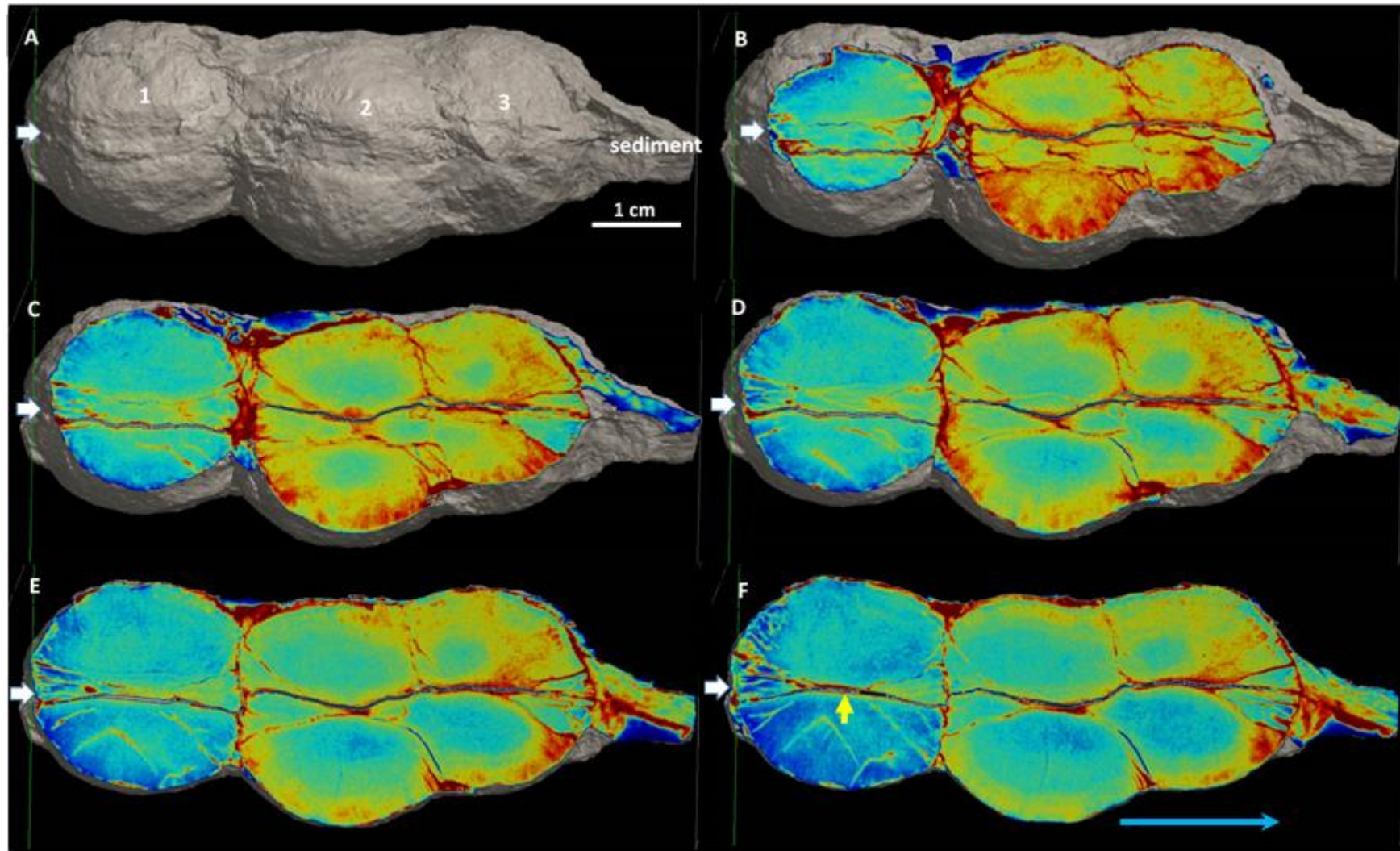


Figure S23: Tomographic views of the 'triple' nodule. (A) Whole. (B-F) Vertical sections from edge to center showing a clear separation between the 'nodule' 1 and the 'nodules' 2 and 3, and an incomplete separation between 'nodule' 2 and 'nodule' 3; Note the evolution of the median disc of the 'nodule' 1 from B to F (white arrow), the communication zone (point) between the two hemispheres appears in (F) (yellow arrow). The blue arrow indicates the growth direction.